Stress Relaxation of End-Linked Polydimethylsiloxane Elastomers with Long Pendent Chains

Ashish Batra, Claude Cohen,* and Lynden Archer

School of Chemical and Biomolecular Engineering, Olin Hall, Cornell University, Ithaca, New York 14853

Received May 3, 2005; Revised Manuscript Received June 15, 2005

ABSTRACT: Two important issues in the area of stress relaxation in elastomers are addressed experimentally in this paper. The first deals with the dependence of the terminal relaxation time on the number of entanglements that a chain tethered to a network makes with the network, and the second deals with the validity of the empirical Chasset−Thirion equation. By carefully end-linking PDMS chains to form networks with few defects besides the controlled amount of long pendent chains, our results show a much weaker exponential dependence of the terminal relaxation time on number of entanglements per tethered chain than predicted by the Doi−Kuzuu theory for a fixed entanglement network but closer to the exponential dependence predicted by lattice calculations with a harmonic potential. The Chasset−Thirion equation is found to hold only in an intermediate time regime of the relaxation spectrum.

1. Introduction

Over the past several decades considerable effort has been devoted to understanding the rheology of star polymer melts.[1−14] The theoretical effort in this field is inspired by models based on the retraction of a branched chain in a fixed network, a mechanism proposed by de Gennes.[2] The Doi−Kuzuu[3] theory for arm retraction in a fixed network predicts that the longest relaxation time τ_m should increase exponentially with the number of entanglements N per star arm and have a power law preexponential factor

$$\tau_m \sim N^{\beta} \exp(\alpha N) \tag{1}$$

where $\beta = 3$ and $\alpha = 15/8$. The detailed theory of Pearson and Helfand[4] predicted $\beta = 1.5$. They found that for a lattice model α depends only on the coordination number q of the lattice and is given by[5]

$$\alpha = \frac{1}{2} \ln\left[\frac{q^2}{4(q-1)}\right] \tag{2}$$

which yields $\alpha = 0.294$ for a cubic lattice. Using Monte Carlo simulations on a cubic lattice, Needs and Edwards[6] estimated $\beta = 1.9$ and $\alpha = 0.195$, but with corrections to account for approximations made to get a true terminal relaxation time, they found $\alpha = 0.31$. Barkema and Baumgaertner[11] revisited lattice simulations over time scales several magnitudes longer than previous simulations and found that $\beta = 2$ and α is the same as predicted by the Pearson and Helfand model. Neither the Doi−Kuzuu theory nor lattice calculations considered the effect of constraint release in which the motion of surrounding chains releases entanglement constraints. Milner and McLeish[9,10] proposed improved dynamic dilution models which predicts star melt rheology fairly accurately. There is some agreement now that $\alpha \approx 0.48$ and $\beta \approx 2.0$ for star polymer melts after correcting for dynamic dilution effects.[14] To our knowledge, no experiment has been performed on cross-linked networks to verify the original theoretical predictions in a fixed network where dynamic dilution effects are suppressed. As stated above, lattice simulations and the traditional tube theory differ substantially in the value of α for a fixed network. Here, we synthesize a series of model end-linked PDMS networks with controlled amounts of pendent chains of different molecular weights. Because the effective molecular weight between cross-links of our networks is either less than or close to the entanglement molar mass (M_e) of PDMS and the amount of added pendent chains is below their entanglement concentration, possible dynamic dilution effects are suppressed. We therefore examine the terminal relaxation time of pendent chains with low polydispersity anchored in a network as a function of the molar mass of the pendent chains to determine the exponent α.

Stress-relaxation of cross-linked polymer elastomers has been the focus of several experimental[15−18] and theoretical studies.[19−25] The polymer networks in these studies are made by random cross-linking such that the cross-link density and molar mass of pendent chains are interdependent parameters. Experimental stress-relaxation data have been found to follow the empirical Chasset−Thirion equation[15] of the power law form

$$G(t) = G_e\left(1 + \left(\frac{t}{\tau_e}\right)^{-m}\right) \tag{3}$$

where $G(t)$ is the stress relaxation modulus, G_e is the equilibrium modulus, and m and τ_e are material parameters. The expression $\tau_e{}^m$ represents the relative unrelaxed stress in excess of the equilibrium stress at $t = 1$ s.[16] Though several models[19−25] proposed in the past support this form for the stress relaxation, the molecular basis of relaxation differs in several of these models. The models can however be grouped into two main categories. In one group, the long time relaxation occurs due to relaxation of pendent chains in an essentially fixed network, and in the other group, the relaxation is due to topological constraint release effects of network strands.

Models based on the retraction of pendent chains in a fixed network have been reviewed and critiqued in detail by McKenna and Gaylord.[26] Curro and Pincus,[19] Thirion and Monnerie,[21] and Curro et al.[20] arrive at a

10.1021/ma050933l CCC: $30.25
Published on Web 07/15/2005

power law form by recognizing that a distribution of pendent chain lengths exist in randomly cross-linked networks. The exponent m in eq 3 is predicted to be proportional to cross-link density (ν) in the Curro and Pincus' model[19] and in the model of Curro et al.[20] Thirion and Monnerie[21] find that m scales as $\nu^{1/3}$. These authors assume the entanglement molecular weight scales as $\nu^{-2/3}$ whereas Curro et al. assume the entanglement molecular weight to be independent of cross-link density. Gaylord et al.[22] use a continuous random walk model to describe the stress relaxation of the pendent chains in randomly cross-linked networks and find that different versions of the random walk model lead to either a power law or a fractional-exponential form for the stress relaxation, neither of which are explicit functions of cross-link density. They also show that both forms fit data for randomly cross-linked natural rubber reasonably well.

Heinrich et al.[23−25] have proposed a single chain approximation for the relaxation due to topological constraint release of the network strands. They argue that the characteristic time $\tau(N)$ of the constraint release process of a single network chain should be same as the exponential law for a melt of branched f-arm star molecules, but with a modified preexponential factor:

$$\tau(N) = \tau_0(N/N_e)^{\mu} \exp(kN/N_e) \qquad (4)$$

where μ is introduced as a fitting parameter to express the higher cooperativity of networks.[23] Values of μ between 3 and 12 are found for different elastomers if experimental creep data are discussed within this model. Their power law expression for the stress relaxation has an exponent that depends directly on the cross-link density (ν) and a time constant similar to the time constant τ_e in eq 3 that is proportional to $\nu^{-\mu}$.

The structure of networks changes considerably with cross-link density in random cross-linking. The relation of stress-relaxation to the structure is thus complicated in these elastomers. To decouple the effect of cross-link density from that of the molecular weight of pendent chains, we have prepared networks by end-linking a mixture of low polydispersity difunctional vinyl-terminated PDMS chains and ∼10 wt % of low polydispersity monofunctional PDMS chains of varying molecular weights using a tetrafunctional cross-linker. Recently Vega et al.[27] studied stress relaxation of end-linked networks containing narrow polydispersity pendent chains of varying molecular weight in a host with a broad molecular weight distribution. The authors find that the Chasset−Thirion equation also holds for the stress relaxation of such networks. These authors use the equilibrium shear modulus as a fitted parameter in eq 3 and show that the stress relaxation of such networks obeys the Chasset−Thirion equation. However, because the equilibrium modulus is left as a fitted parameter, the validity of the empirical equation at long times remains untested. In this paper, we examine the validity of the empirical equation by measuring the terminal relaxation modulus of the networks and establish a proper methodology for analysis using eq 3. We vary the cross-link density independently and point out the limitations with both high cross-link and low cross-link density "model" elastomers in testing the validity of the Chasset−Thirion equation and in determining the exponential scaling of the terminal relaxation of pendent chains.

Table 1. Molecular Weights of PDMS Precursors

polymer chains	M_n (kg/mol)	PDI
Difunctional Chains (B_2)		
I	7.5	1.18
II	24	1.33
Monofunctional Chains (B_1)		
I	33	1.24
II	54	1.18
III	86	1.28
IV	119	1.31
V	147	1.32
VI	206	1.25
VII	242	1.20

2. Experimental Procedures

2.1. PDMS Samples. Low polydispersity bifunctional vinyl-terminated PDMS precursor chains (B_2) were synthesized from hexamethylcyclotrisiloxane (D_3) monomer (Gelest, Inc.) by anionic ring-opening polymerization in a 50 wt % toluene solution at 60 °C using benzyltrimethylammonium bis(*o*-phenylenedioxy)phenylsiliconate as a catalyst and dimethyl sulfoxide (DMSO) as a promoter. Calculated amounts of water were added to control the molecular weight of the resulting polymer. After the polymerization, pyridine, an acid scavenger, was added to the resulting polymer/toluene mixture. The living chains were end-capped with vinyl groups by adding vinyldimethylchlorosilane. The polymer samples thus obtained were washed with water, dissolved, reprecipitated with toluene and methanol, and then dried in a vacuum oven at 60 °C for 3 days. The details of the catalyst preparation and synthesis of polymer are reported elsewhere.[28−31] Monofunctional vinyl-terminated PDMS precusor chains (B_1) were synthesized by polymerizing D_3 in a 50 wt % solution of cyclohexane at 33 °C, using *n*-BuLi as an initiator and DMSO as a promoter. Calculated amounts of 1.6 M solution of *n*BuLi in hexane were added to control the molecular weight of B_1. The monofunctional B_1 was end-capped, washed, and dried using the same methods as for the preparation of B_2. High polydispersity B_1 samples were fractionated using a toluene/methanol system. Both B_2 and B_1 were characterized using gel permeation chromatography in toluene, and the results are reported in Table 1. Networks were formed by end-linking with the tetrafunctional cross-linker tetrakis(dimethylsiloxy)silane in the presence of a platinum catalyst. The optimum amount of cross-linker tetrakis(dimethylsiloxy)silane (A_4) was added to the polymer mixture, and the reaction was catalyzed by *cis*-dichlorobis(diethyl sulfide)platinum(II) in toluene. On the basis of a previous study,[31] the optimal molar ratio r of silane hydrogens to vinyl groups was fixed at 1.7 for all networks considered here. The networks were allowed to cure at 35 °C for 3 days. The weight fraction of soluble material, w_{sol}, and the equilibrium swelling ratio in toluene, Q, were determined using standard gravimetric procedures.[32] Network characteristics are reported in Table 2. The first roman numeral corresponds to the B_2 chains, and the second number corresponds to the B_1 chains. B_2 I−IV, for example, implies a host network made from B_2 I chains with added B_1−IV pendent chains.

2.2. Stress Relaxation under Shear. The degassed reactive mixture of B_1, B_2, A_4 and the catalyst were placed between the cone (4° and 15 mm diameter) and plate of a Paar Physica MCR-300 rheometer and allowed to cure overnight at 25 °C. A dynamic frequency sweep between 0.01 and 100 rad/s was carried out at 25 °C to characterize the storage and loss moduli. Simple shear stress relaxation experiments were carried out at 25 °C with deformations within the linear viscoelastic regime. Typically a strain of 10% was used.

3. Results and Discussion

3.1. Stress Relaxation. Figures 1 and 2 show the storage moduli as a function of frequency normalized by their values at 0.01 rad/s for the B_2 I and B_2 II network series at a temperature of 25 °C. Insets in

Table 2. Experimental Characteristics of PDMS Networks

network	w_{sol} (%)	Q	$G(\omega=0.01)/RT$ (mol/m^3)	G_e/RT	G_e (MPa)
B_2 I			150.8	150.8	0.373
B_2 I−I			107.4	109.1	0.270
B_2 I−II			121.5	120.5	0.298
B_2 I−III	1.61	3.33	136.5	136.2	0.337
B_2 I−IV	2.02	3.20	122.8	122.0	0.302
B_2 I−V	1.50	3.31	138.7	137.2	0.339
B_2 I−VI	1.35	3.36	137.7	135.2	0.334
B_2 I−VII	1.29	3.48	131.6		
B_2 II			95.5	94.5	0.234
B_2 II−I			85	84.1	0.208
B_2 II−II			83.2	82.5	0.204
B_2 II−III	1.50	4.06	81.6		
B_2 II−IV	1.69	4.09	85.5		
B_2 II−V	1.69	4.16	91.5		
B_2 II−VI	1.58	4.21	90.9		
B_2 II−VII	1.29	4.09			

Figures 1 and 2 show that the storage modulus becomes nearly independent of frequency at low frequencies. For the same host network series, the values of the storage moduli at a frequency of 0.01 rad/s do not vary much with the molecular weight (M_n) of the pendent chains (see Table 2), supporting the assumption that the networks made from the same precursor chains have similar cross-link density. It is clear from Figures 1 and 2 that as the number of entanglements per pendent chain, N, obtained from the ratio of M_n to M_c (the molecular weight between effective cross-links (M_c) is calculated as $\rho RT/G_e$ where ρ is the density of the network and G_e is the equilibrium shear modulus) increases, the storage modulus at high frequencies increases. This is because the pendent chains have not relaxed, and their entanglements with the networks contribute to G' at these frequencies. Figure 1 also shows the storage modulus of an optimal network with minimal defects made from only difunctional B_2 I chains using an optimal nonstoichiometric amount of cross-linker as determined previously.[31] As seen in Figure 1, the storage modulus for the optimal B_2 I network shows no variation in modulus as a function of frequency. Using the Macosko−Miller[31,33] model, we can estimate the fraction of native pendent chains in addition to added pendent chains for networks with known soluble fraction values. For typical w_{sol} shown in Table 2 the total $w_{pen} \sim 0.22$, implying that the native host $w_{pen} \sim 0.12$. Even optimal networks synthesized from purely difunctional chains have ~10% of host pendent chain defects.[34] It has been shown previously[34] that ^{2}H NMR transverse dephasing measurements provide a better estimate of elastic chain contribution and consistently predict a lower fraction of pendent chains than the Macosko−Miller model, and estimates of pendent chain fraction from the model should be regarded as upper bounds. In the case of the B_2 I network series, the relaxation of these small host pendent chains is very fast compared to the added pendent chains that have at the very least around 4 times the molar mass of the host precursor chains. The amount of added pendent chains (10% weight fraction) corresponds to just $0.31\phi_e$ (for a 54K PDMS chain) and $0.94\phi_e$ (for a 242K PDMS chain), where ϕ_e represents the concentration at which entanglements between the pendent chains becomes important.[35] The number of entanglements that a pendent chain makes with the network can then be determined by the mesh size of the network (M_c). On the other hand, in the case of the B_2 II network series

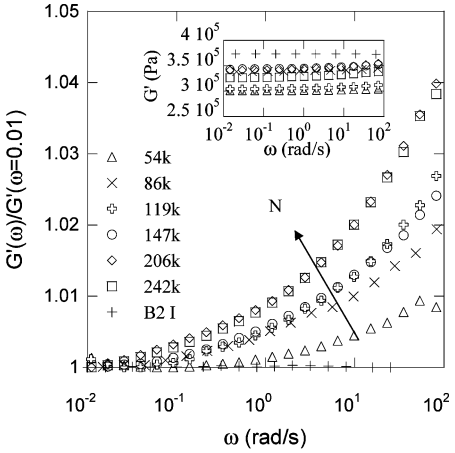

Figure 1. Storage moduli at 298 K as a function of frequency (ω) normalized by their value at $\omega = 0.01$ rad/s for B_2I host with 10 wt % pendent chains of increasing molecular weight. In the inset are the storage moduli as a function of frequency.

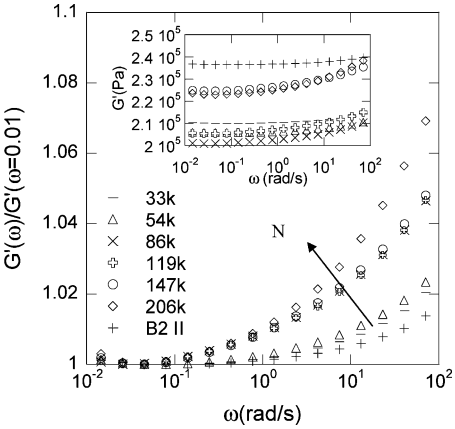

Figure 2. Storage moduli at 298 K as a function of frequency (ω) normalized by their value at $\omega = 0.01$ rad/s for B_2 II host with 10 wt % pendent chains of increasing molecular weight. In the inset are the storage moduli as a function of frequency.

the native pendent chains are long enough to prevent a simple analysis that assumes that stress relaxation occurs primarily due to arm retraction of the added pendent chains in a fixed network. As shown in Figure 2, the storage modulus of the optimal B_2 II network synthesized with no monofunctional chains does increase with frequency as the native pendent chains are long enough to entangle with the network.

Figures 3 and 4 show the normalized curves for the stress-relaxation modulus $G(t)/G(0.01)$ of the B_2 I and B_2 II network series, respectively. The time to reach a strain of 10% is 0.11 s in all our experiments. $G(t = 0.01$ s) refers to first measurement of G after the initial 0.11 s to impose the strain. The optimal B_2 I network shows no relaxation whereas the optimal B_2 II network shows some relaxation as explained earlier.

The Chasset−Thirion equation is usually employed to fit to stress-relaxation curves of elastomers. This is a three-parameter (m, τ_e, and G_e) equation and some comments on the proper fitting procedure are in order. G_e or the equilibrium shear modulus can in principle be measured from the steady-state value of $G(t)$ obtained from stress relaxation experiments in the terminal relaxation regime. But G_e has been used as a fitting parameter in the literature, thereby preventing a rigorous test of the equation itself. For most of the samples of the B_2 I series and two samples of the B_2 II series,

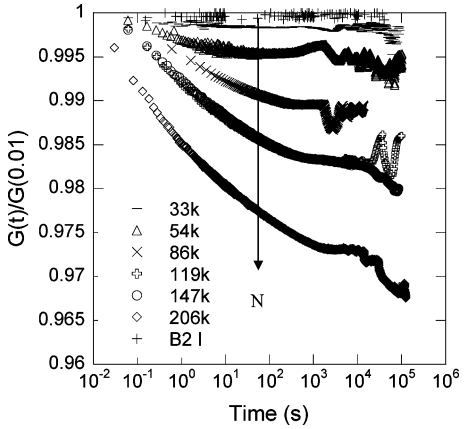

Figure 3. Normalized stress-relaxation modulus $G(t)/G(0.01)$ as a function of time at 298 K for B_2 I sample and B_2 I samples with 10 wt % of different B_1 pendent chains.

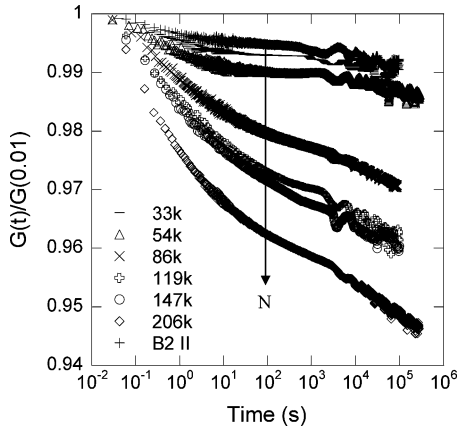

Figure 4. Normalized stress-relaxation modulus $G(t)/G(0.01)$ as a function of time at 298 K for B_2 II and B_2 II samples with 10 wt % of different B_1 pendent chains.

the equilibrium relaxation modulus was reached before the onset of transducer drift (Figures 3 and 4). In other samples, a transducer drift occurs before reaching the equilibrium modulus. For the two samples of the B_2 II series with the lowest M_w pendent chains where the terminal relaxation modulus has been achieved (Figure 4), an analysis of the data is complicated by the fact that native pendent chains (see data for sample B_2 II with no added pendent chains) are also relaxing on the same time scale as the added pendent chains.

In Figure 5 we plot $\log(G(t)/G_e - 1)$ vs logt for the B_2 I network series. It is evident from this figure that a power law is obeyed only over a very limited time span. A similar data analysis procedure has been used by Dickie and Ferry.[16] But, they choose a value of G_e by trial and error that produces a linear plot. The slope of this plot gives m and τ_e is obtained from the value of the ordinate at $t = 1$ s. Figure 6 is a blowup of the power law region. Table 3 lists the values of m and τ_e for the B_2 I series obtained from straight line fits to these data. However, one must note that in previous studies G_e is typically 75−80% of the initial value $G(0)$, and an equilibrium modulus within an accuracy of ±1% would suffice. Here G_e is within 5% of $G(0)$, and an analysis such as that presented in Table 3 is therefore valid only for samples for which a G_e value can be predicted to an accuracy of ±0.1% or better. A 0.2% change in G_e, for example, can cause a 20−30% change in the value of m. In this study such accuracy is possible only for B_2 I−I, B_2 I−II, B_2 I−IV, B_2 I−V, and B_2 I−VI networks,

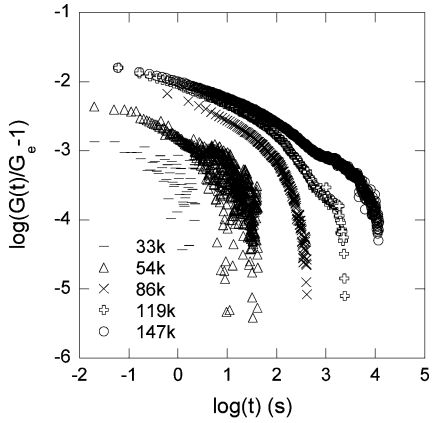

Figure 5. $(G(t)/G_e - 1)$ vs t for B_2 I host with 10 wt % of different B_1 pendent chains.

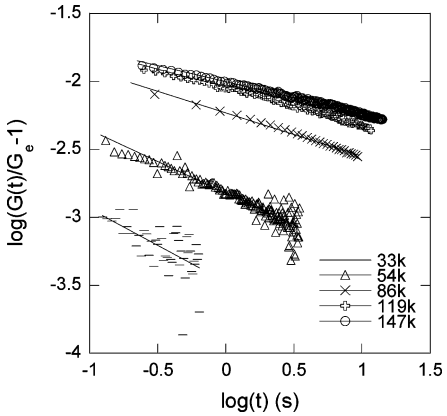

Figure 6. $\log(G(t)/G_e - 1)$ vs $\log t$ for B_2 I host with 10 wt % of different B_1 pendent chains.

Table 3. Fitted Parameters of Chasset−Thirion Equation for the Shear Stress Relaxation of PDMS Networks

network	N	m	τ_e (s)	$G_e/G(0.01)$
B_2 I−I	4	0.53	6.3×10^{-4}	0.9983
B_2 I−II	7	0.46	3.3×10^{-3}	0.9953
B_2 I−III	12	0.32	1.85×10^{-2}	0.9895
B_2 I−IV	15	0.272	3.3×10^{-2}	0.9820
B_2 I−V	21	0.23	4.1×10^{-2}	0.9757

and the results are reported in Table 3. Table 2 shows the extremely small differences in the value of $G(0.01$ rad/s$)/RT$ vs G_e/RT for these networks. Based on these values of G_e, the average M_c for B_2 I network series is around 7.8K.

As has been correctly pointed out by McKenna et al., a log−log representation of the transient term $r(t) = G(t)/G_e - 1$ vs time is the best representation to determine the validity of the Chasset−Thirion equation. Often, the Chasset−Thirion equation seems to fit to the entire time range of stress-relaxation curves with a three-parameter fit on a semilog plot of $G(t)$ vs time.[27,36] In Figure 7 we plot m vs N and find $m \sim N^{-(0.55\pm0.05)}$. In a recent study,[27] a model for the stress relaxation of end-linked networks with pendent chains was developed. The model is an extension of the Curro−Pincus[19] model but with a log−normal distribution of pendent chain lengths instead of the geometric distribution of pendent chain lengths appropriate for random cross-linking. On the basis of both the theoretical model and experimental results for networks of a single mesh size, the authors reported that the power law exponent m is inversely related to M_w, the mass average molar mass of the pendent chains.[27]

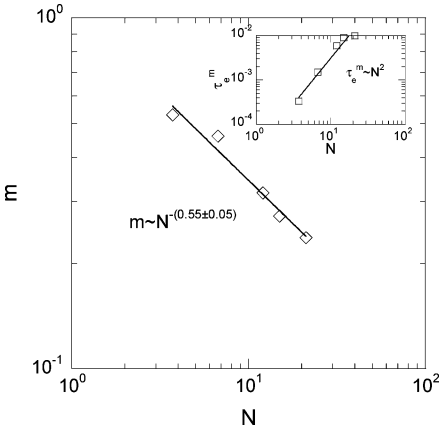

Figure 7. m vs N for B_2 I network series with 10 wt % of different B_1 pendent chains. In the inset is $\tau_e{}^m$ vs N for B_2I networks series.

Though Curro et al.[6] have shown that τ_e is related to τ_o, the maximum Rouse relaxation time of a pendent chain with molar mass equal to the entanglement molar mass, one cannot attach a physical meaning to τ_e in the power law form of eq 3 besides the one given earlier as the relative unrelaxed stress in excess of equilibrium at 1 s. We plot $\tau_e{}^m$ vs N in the inset of Figure 7. The value of $\tau_e{}^m$ is equal to $(G(1)/G_e - 1)$ and represents the relative unrelaxed stress in excess of the equilibrium value at an elapsed time of 1 s in a stress relaxation experiment. We find that $\tau_e{}^m$ scales as N^2. For randomly cross-linked samples, Dickie and Ferry found $\tau_e{}^m$ to scale as ν^2, where ν is the cross-link density.

3.2. Terminal Relaxation Time. The physically relevant terminal relaxation time could in principle be obtained from master curves for the loss modulus of each sample by performing frequency sweeps between 0.002 and 100 rad/s at temperatures ranging from 0 to 200 °C and using a time−temperature superposition. We have attempted to generate such master curves, but the low-frequency response was either very noisy reaching the limits of the sensitivity of the instrument (for the smaller molecular weight pendent chains) or the terminal relaxation regime could not be accessed in this temperature range (for the higher molecular weight pendent chains). Temperatures higher than 200 °C could not be used due to irreversible changes to the samples at such high temperatures.

To determine the average terminal relaxation time in series B_2 I, we resorted to plotting $t(G(t)/G_e - 1)$ vs t curves shown in Figure 8. These curves are normalized by the maximum value of $t(G(t)/G_e - 1)$ for each network. A plot of $t(G(t)/G_e - 1)$ vs t will show a maximum at the average relaxation time, provided $g(t) = \sum_i g_i \exp(-t/\tau_i)$, where $g(t) = G(t)/G_e - 1$. For a maxima in the function $tg(t)$ the first derivative of $tg(t)$ must be zero, implying

$$\frac{\partial}{\partial t}(tg(t)) = \sum_i g_i \left(1 - \frac{t_{max}}{\tau_i}\right) \exp\left(-\frac{t_{max}}{\tau_i}\right) = \hat{g}(t_{max}) = 0 \quad (5)$$

Since the exponential term corresponding to the slowest mode makes the largest contribution to $\hat{g}(t_{max})$, so the condition $\hat{g}(t_{max}) = 0$ implies $t_{max} = \hat{\tau}_m$, where $\hat{\tau}_m$ is the average terminal relaxation time subsequently referred to as τ_m. To extract this value of τ_m, the data in Figure 8 are fitted to $At \exp(-t/\tau_m)$ with A and τ_m as the fitting

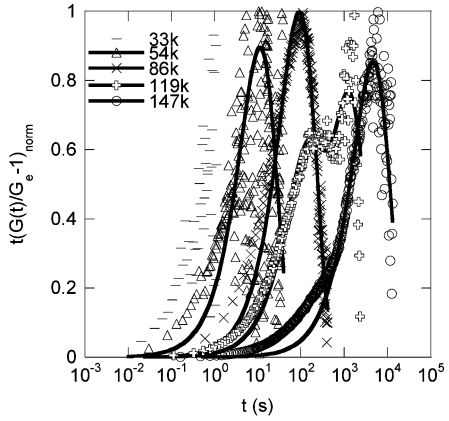

Figure 8. $t(G(t)/G_e - 1)_{norm}$ vs t for B_2 I network series with 10 wt % of different B_1 pendent chains.

Table 4. Values of the Terminal Relaxation Time for the B_2 I Network Series

network	N	τ_m (s) (fit)	τ_m (s) (peak position)
B_2 I−I	4		1
B_2 I−II	7	11.3	3
B_2 I−III	12	91.3	105
B_2 I−IV	15	1243.6[a]	1700
B_2 I−V	21	4658.9	4500

[a] Using a double-exponential fit gives 110 and 1243.6 s as values of the two relaxation times. A single exponential gives a value of 742.4 s.

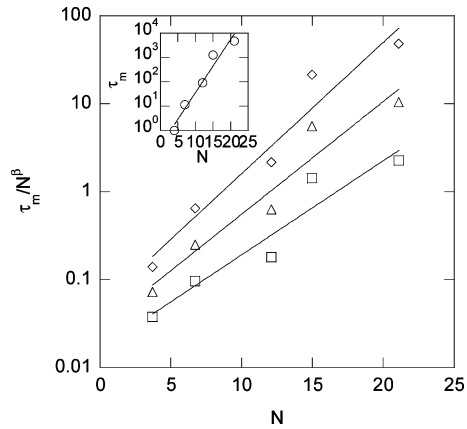

Figure 9. τ_m/N^β vs N for the B_2 I network series. Lines are fits to $\exp(\alpha N)$ with $\beta = 1.5$ (◇), $\beta = 2$ (△), and $\beta = 2.5$ (□). Inset shows the exponential dependence of τ_m vs N.

parameters. For the B_2 I−I network, data are too noisy to fit, and the value of τ_m is read off as an approximate value where the peak seems to appear, but for B_2 I−III, B_2 I−IV, and B_2 I−V, good fits are obtained with the above-mentioned function. For the B_2 I−IV pendent chains, a double-exponential fit has also been used to illustrate that the long relaxation time is close to the value predicted by a single exponential. Table 4 shows the values of τ_m obtained from fits as well as those estimated by peak positions in Figure 8.

In Figure 9 we examine the dependence of τ_m on N on the basis of eq 1 by plotting τ_m/N^β vs N. Here the values of τ_m obtained by the fitting procedure described above have been used. Given the limited number of data points, a two-parameter fit to get both α and β would not be statistically meaningful. Hence, we choose to fix the value of β to 1.5, 2, or 2.5 as proposed by various theories.[4,8,37] It is evident that the dominant behavior is an exponential dependence on the number of en-

tanglements per pendent chain. Within experimental error, the value of α is determined to be 0.34 ± 0.04 for $\beta = 1.5$, 0.3 ± 0.03 for $\beta = 2$, and 0.26 ± 0.027 for $\beta = 2.5$. If the value of τ_m determined by the peak position is used, the value of α is found to be 0.42 ± 0.13 for $\beta = 1.5$, 0.37 ± 0.13 for $\beta = 2$, and 0.34 ± 0.12 for $\beta = 2.5$. The deviation values are obtained by fitting to various subsets of the data presented in Table 4. These values of α are evidently much weaker than 1.5 predicted by the Doi−Kuzuu theory[3] and are overall close to the value of 0.3 determined in lattice models with quadratic potentials.[38,39] We discuss below the assumptions of these models.

Arm retraction by a distance along the contour of the tube in the tube models of Doi and Kuzuu has been analyzed as a thermally activated process in an effective potential approximated by the quadratic potential

$$U(s) = \nu' NkT\left(1 - \frac{s}{L_{eq}}\right)^2 \tag{6}$$

where ν' in this equation is identified as the α used in this paper. For Gaussian chain statistics ν' was found to be 1.5. The quadratic potential and the related Gaussian probability distribution of tube length L for a chain with N_a monomers are valid at least in principle, only for small tube length fluctuations. Lattice models have shown that this potential is nonquadratic and differs significantly from the form of eq 6 for the deep fluctuations required to achieve terminal relaxation. This brings into question the validity of identifying ν' in these models with the α of eq 1.

In the 1980s a number of authors[5,38−41] considered the model of a "polymer chain on a regular lattice of obstacles". In these models it was assumed that a polymer chain strongly entangled with other chains could be represented as a random walk among obstacles forming the lines of a spatial lattice. Pearson and Helfand[5] and subsequently Khokhlov and Nechaev[40] presented exact solutions for the case in which the step size of the random walk "*a*" is equal to the distance "*c*" between obstacles. Rubinstein and Helfand[38] presented results on a 2D lattice for the more general case of $c > a$ with values of c/a between 1 and 10. They found values of α to vary between 0.333 for $c/a = 1$ and 0.2026 for $c/a = 10$ for the case of small fluctuations of polymer ends in a tube that could be represented by the quadratic potential. For large contractions for which the probability distribution of the tube length L deviates from the Gaussian form, but still under assumption of a quadratic potential, they find α to vary between 0.287 for $c/a = 1$ to 0.246 for $c/a = 10$. The most general case of a 3D cubic lattice was treated by Zheligovskaya et al.[39] For small fluctuations and a quadratic potential α varies from 0.6 for $c/a = 1$ to 0.16 for $c/a = 64$. But for large fluctuations and without approximating the potential to be quadratic, they find α to vary from 3.403 to 0.85.

Rubinstein and Colby[35] have mapped the parameter c/a to the physically relevant number of monomers in an entanglement strand N_e. For the PDMS B_2 I network series, the average number of monomers N_c between effective cross-links equals 21. Using Table 1 of ref 39 and Figure 9.14 of ref 35, one can read off a value of α ≈ 0.31 for small fluctuations in a quadratic potential and a value of 1.6 for large fluctuations in a nonquadratic potential for a N_c of ∼21. Recently, Shanbhag and Larson[42] have analyzed primitive paths obtained using the bond fluctuation model for chains up to 12.5 entanglements. They find a quadratic potential with a value close to 1.5. They do observe some decrease in the value of α with increasing N, which indicates that the value of α might not be unique for a large range of N but there could be certain ranges of N over which a particular value of α would work best.

To summarize, there is still considerable theoretical uncertainty about the appropriate assumptions with regard to small vs large fluctuations or with regard to the appropriate potential to be used for arm retraction of isolated arms in a network. Our experimental results seem to match most closely the predictions of a quadratic potential on a 3D lattice. However, it is unclear why this should be the case unless we can argue that the values of N (up to 20) examined in our experiments are not large enough to cause appreciable deviations from a quadratic potential or that the quadratic potential is indeed valid for large values of N.

4. Conclusions

We have synthesized end-linked PDMS networks with controlled amounts of fairly narrow molecular weight distribution pendent chains that are added to networks with host chains with varying effective molecular weight between cross-links. The goal was twofold. One, to determine whether the theoretical prediction of a strong exponential dependence of the terminal relaxation time with the number of entanglements per star arm in a fixed entanglement network was valid. We find a much weaker dependence that compares favorably to the 3D lattice calculations of Zheligovskaya et al.[39] in a quadratic potential. Second, we find that the stress relaxation moduli under shear can be fitted only in a limited time span by the Chasset−Thirion equation. The exponent m is found to be inversely proportional to the number of entanglements of the pendent chains but with a weaker dependence of 0.55. The relative unrelaxed stress in excess of equilibrium at 1 s is found to scale as N^2. We illustrate the reasons why only certain cross-link density samples can be used to carry out model stress-relaxation studies. Networks end-linked with $M_n < 7.5$K result in stress relaxation too small to resolve accurately with mechanical rheometers. Networks with $M_n > 15$K are complicated by similarities in lengths of native pendent chains and added pendent chains.

Acknowledgment. This work was supported by the NSF Polymers Program under Grant DMR-0349952. We acknowledge useful discussions with G. B. McKenna, T. M. Duncan, F. Escobedo, and D. Bhawe.

References and Notes

(1) Kraus, G.; Gruver, J. T. *J. Polym. Sci.* **1965**, *A3*, 105.
(2) de Gennes, P. G. *Scaling Concepts in Polymer Physics*; Cornell University Press: Ithaca, NY, 1979.
(3) Doi, M.; Kuzuu, N. *J. Polym. Sci., Polym. Phys. Ed.* **1980**, *18*, 775.
(4) Pearson, D. S.; Helfand, E. *Macromolecules* **1984**, *17*, 888.
(5) Helfand, E.; Pearson, D. S. *J. Chem. Phys.* **1983**, *79*, 2054.
(6) Needs, R. J.; Edwards, S. F. *Macromolecules* **1983**, *16*, 1492.
(7) Ball, R. C.; McLeish, T. C. B. *Macromolecules* **1989**, *22*, 1911.
(8) Fetters, L. J.; Kiss, A. D.; Pearson, D. S.; Quack, G. F.; Vitus, F. J. *Macromolecules* **1993**, *26*, 647.
(9) Milner, S. T.; McLeish, T. C. B. *Macromolecules* **1997**, *30*, 2159.

(10) Milner, S. T.; McLeish, T. C. B. *Macromolecules* **1998**, *31*, 7479.
(11) Barkema, G. T.; Baumgaertner, A. *Macromolecules* **1999**, *32*, 911.
(12) Shanbhag, S.; Larson, R. G.; Takimoto, J.-I.; Doi, M. *Phys. Rev. Lett.* **2001**, *85*, 195502.
(13) Watanabe, H.; Matsumiya, Y.; Inoue, T. *Macromolecules* **2002**, *35*, 2339−2357.
(14) Vega, D. A.; Sebastian, J. M.; Russel, W. B.; Register, R. A. *Macromolecules* **2002**, *35*, 169.
(15) Chasset, R.; Thirion, P. In *Proceedings of the Conference on Physics of Non-Crystalline Solids*; Prins, J. A., Ed.; North-Holland Publishing Co.: Amsterdam, 1965.
(16) Dickie, R.; Ferry, J. D. *J. Phys. Chem.* **1966**, *70*, 2594.
(17) Plazek, D. J. *J. Polym. Sci., Part A-2* **1966**, *4*, 745.
(18) Arenz, R. J. *J. Polym. Sci., Polym. Phys. Ed.* **1974**, *12*, 131.
(19) Curro, J. G.; Pincus, P. *Macromolecules* **1983**, *16*, 559.
(20) Curro, J. G.; Pearson, D. S.; Helfand, E. *Macromolecules* **1985**, *18*, 1157.
(21) Thirion, P.; Monnerie, L. *J. Polym. Sci., Part B: Polym. Phys.* **1986**, *24*, 2307.
(22) Gaylord, R. J.; Weiss, G.; Di Marzio, E. *Macromolecules* **1986**, *19*, 927.
(23) Heinrich, G.; Vilgis, T. A. *Macromolcules* **1992**, *25*, 404.
(24) Heinrich, G.; Havránek, A. *Prog. Colloid Polym. Sci.* **1988**, *78*, 1.
(25) Havránek, A.; Heinrich, G. *Acta Polym.* **1988**, *39*, 563.
(26) McKenna, G. B.; Gaylord, R. *Polymer* **1988**, *29*, 2027.
(27) Vega, D. A.; Villar, M. A.; Alessandrini, J. L.; Valles, E. M. *Macromolecules* **2001**, *34*, 4591.
(28) Lee, C. L.; Marko, O. W.; Johannson, O. K. *J. Polym. Sci., Polym. Chem. Ed.* **1976**, *14*, 743.
(29) Lee, C. L.; Johannson, O. K. *J. Polym. Sci., Polym. Chem. Ed.* **1976**, *14*, 729.
(30) Lee, C. L.; Frye, C. L.; Johannson, O. K. *Polym. Prepr., Am. Chem. Soc. Div. Polym. Chem.* **1969**, *10*, 1361.
(31) Patel, S. K.; Malone, S.; Cohen, C.; Gillmor, J.; Colby, R. *Macromolecules* **1992**, *25*, 5241.
(32) Weiss, P.; Hild, G.; Herz, J.; Rempp, P. *Makromol. Chem.* **1970**, *135*, 249.
(33) Macosko, C. W.; Miller, D. R. *Macromolecules* **1976**, *9*, 199. (b) Miller, D. R.; Macosko, C. W. *Macromolecules* **1976**, *9*, 206. (c) Miller, D. R.; Valles, E. M.; Macosko, C. W. *Polym. Eng. Sci.* **1979**, *19*, 272.
(34) McLoughlin, K.; Szeto, C.; Duncan, T. M.; Cohen, C *Macromolecules* **1996**, *29*, 5475.
(35) Rubinstein, M.; Colby, R. H. *Polymer Physics*; Oxford University Press: New York, 2003; pp 369−377.
(36) Roth, L. E.; Vega, D. A.; Vallés, E. M.; Villar, M. A. *Polymer* **2004**, *45*, 5923.
(37) Frischknecht, A. L.; Milner, S. T. *Macromolecules* **2000**, *33*, 9764.
(38) Rubinstein, M.; Helfand, E. *J. Chem. Phys.* **1985**, *82*, 4387.
(39) Zheligovskaya, E. A.; Ternovskii, F. F.; Khokhlov, A. R. *Theor. Math. Phys.* **1988**, *75*, 644.
(40) Khokhlov, A.; Nechaev, S. *Phys. Lett. A* **1985**, *112*, 156.
(41) Nechaev, S.; Semenov, A.; Koleva, M. *Physica A* **1986**, *140*, 506.
(42) Shanbhag, S.; Larson, R. G. *Phys. Rev. Lett.* **2005**, *94*, 076001.

MA050933L